Available online at www.sciencedirect.com

SCIENCE DIRECT®

Solid State Ionics 175 (2004) 851–855

SOLID STATE IONICS

www.elsevier.com/locate/ssi

Ionic conduction in LiI–α,γ-alumina: molecular dynamics study

R.W.J.M. Huang Foen Chung*, S.W. de Leeuw

Department of Applied Physics, Delft University of Technology, Lorentzweg 1, 2628 CJ Delft, The Netherlands

Abstract

Molecular dynamics simulations were performed on LiI–α,γ-alumina. The LiI–α,γ-alumina systems were constructed by sandwiching a LiI crystal between respectively two α- and two γ-alumina crystals. Two interfaces were formed by the LiI (001), (002) and the α-alumina (0001) and γ-alumina (001) planes. Structural, vibrational and transport properties of the Li^+ ions in the bulk as well as at the interfaces were investigated. A fraction of Li^+ ions migrated towards the alumina surfaces occupying tetrahedral sites near the interfaces. An increase in the ionic mobility was observed which was mainly caused by the diffusion along the interfaces. The density of Li^+ ions near the α-alumina surfaces was larger than at the γ-alumina surfaces. The charged layer composed by the Li^+ ions on the alumina surfaces results in a net enhanced electric field perpendicular to the interfaces. The migration of Li^+ ions to the alumina surfaces leads to a higher concentration of vacancies in the LiI crystal and gives therefore an increased ionic mobility. The mechanism of diffusion was the same for the LiI–α-alumina interface as well as the LiI–γ-alumina interface. This explains the fact that the activation energy was the same, 0.38 eV. The relatively larger fraction of Li^+ ions which has moved to the α-alumina surfaces leads to a higher pre-exponential factor for the LiI–α-alumina interfaces than for the LiI–γ-alumina interfaces.

Keywords: LiI–α,γ-alumina; Molecular dynamics; Ionic conductivity

1. Introduction

The ionic conductivity of many conductors can be increased considerably by adding a second-phase non-conducting material like for instance SiO_2 or Al_2O_3 through heterogeneous doping. The largest enhancements of the conductivity have been observed in alkali- and alkaline-earth halides such as LiI and the superionic conductor AgI [1–3].

Even though agreement has been reached that the ionic conductivity enhancement is caused by the larger diffusion along the interfaces formed by the conductor and the nonconducting phase, the conduction mechanism itself is not yet fully understood. The space charge model introduced by Jow and Wagner [4] and further developed by Maier [5–7] has been used frequently to explain the interface effects. According to this model, charge carriers move from the ionic conductor to the interface of the second-phase insulator because of the presence of preferential sites at the interface. This charge layer is then compensated by the formation of a layer of charged point defects which leads to the high ionic conductivity. For a number of composite systems, this model explains the conductivity enhancement in a satisfactory manner.

However, according to Dudney's calculations [8], the conductivity enhancement in systems like LiI and AgI cannot be fully attributed to the space charge effects. Lubben and Modine [9], for instance, found no enhancement due to space charge layer formation at the film/substrate interface of LiI/Al_2O_3.

We have performed molecular dynamics simulations of LiI/Al_2O_3 to study space charge effects. Alumina in the α- and γ-phase was used as second-phase insulators. Structural and vibrational properties were examined by determining the Li^+ distribution in the z-direction ([001] LiI crystal direction) perpendicular to the conduction plane (ZDF), the radial distribution function (RDF) and the density of states (DOS) from the normalized velocity auto correlation function (VACF). To search for space charge regions, the

* Corresponding author.

0167-2738/$ - see front matter © 2004 Published by Elsevier B.V.
doi:10.1016/j.ssi.2004.09.047

average total electric field function (EF) was measured. The diffusion coefficient obtained from the mean square displacement (MSD) of the Li^+ ions was determined to study the ionic conductivity.

2. Simulation details

The hybrid model potential function, U, consists of the potential proposed by Deppe [10] for LiI and the potential used by Blonski and Garofalini [11,12] for alumina and can be written as a sum of a two-body and a three-body potential as

$$U = \sum_{\langle ij \rangle} U_2(r_{ij}) + \sum_{\langle ijk \rangle} U_3\left(\vec{r}_{ij}, \vec{r}_{ik}\right). \quad (1.1)$$

Here $r_{ij} = |\vec{r}_i - \vec{r}_j|$, where $\vec{r}_i$ and $\vec{r}_j$ are respectively the position vectors of particle i and j, $U_2(r_{ij})$ is the two-body potential and $U_3\left(\vec{r}_{ij}, \vec{r}_{ik}\right)$ the three-body interaction potential. The two-body potential consists of a Coulomb interaction, exponential repulsion, modified Born–Mayer, dispersive, quadrupole–dipole and a Born repulsive term. The three-body potential includes only the Al–O–Al and O–Al–O nearest neighbour interactions which is denoted by $\langle ijk \rangle$ in Eq. (1.1) in the triple summation. A detail description of the potentials and their adjustable parameters can be found in Refs. [10–12].

The simulation samples were thermalised for 200 ps without sintering (hot-pressing process). Constant temperature simulations were carried out using a Nosé–Hoover thermostat and a velocity-Verlet integration scheme with a timestep of 1.0 fs. Coulombic forces were determined by the iterative PPPM method [13].

3. Results

3.1. Structural properties

In Figs. 1 and 2, the Li^+ distribution in the z-direction perpendicular to the interfaces ([001] direction) of respectively LiI/α-Al_2O_3 and LiI/γ-Al_2O_3 are presented. The ZDF was determined as

$$\mathrm{ZDF}(z) = \left\langle \sum_{i_{\mathrm{Li}}}^{N_{\mathrm{Li}}} \frac{\delta(z - z_{i_{\mathrm{Li}}})}{N_{\mathrm{Li}}} \right\rangle. \quad (1.2)$$

Here i_{Li} denotes a Li^+ ion i and N_{Li} the total number of Li^+ ions. The borders of the interfaces or depleted regions are marked by the dashed lines and the numbers 1, 2, 3, 4, 5 and 6 above the peaks denote the layers which belong to the interfaces and contain Li^+ ions. A fraction of the Li^+ ions migrated from the layers 2, 3, 4 and 5 to the alumina surfaces. This results in the formation of the layers 1 and 6 where the Li^+ are attached to the alumina surface. The vacant sites in the layers 2, 3, 4 and 5 are not ordered and

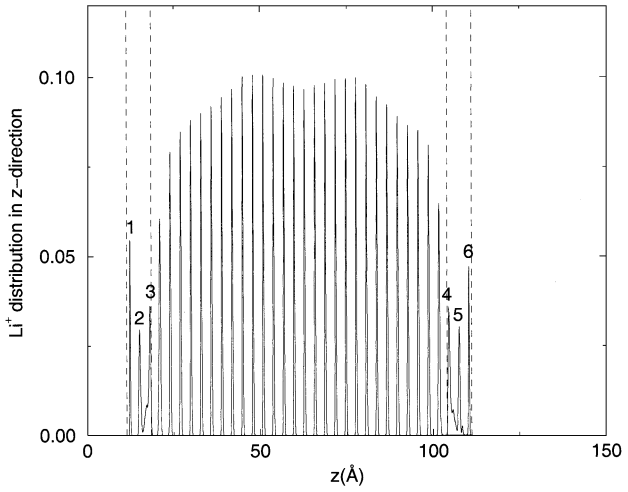

Fig. 1. Li^+ ZDF in LiI/α-Al_2O_3 (300 K). The dashed lines denote the depleted regions while the numbers 1–6 its Li^+ layers.

have rather a liquid-like structure. Through integration of the ZDFs, we determined that the average number of density of Li^+ attached to respectively each α- and γ-alumina surface is 0.0277 and 0.0196 $Å^{-2}$. Integration has shown furthermore that except for the numbered layers, no Li^+ ions have migrated to the alumina surface from the other layers. The majority of the Li^+ came from the layers 2 and 5. An energy calculation reveals that moving one Li^+ ion from layer 2 or 5 to its nearest vacant site at the α-alumina surface, in a perfect crystalline LiI–α-alumina system, gives a decrease of the total energy of ≈5 eV. A similar calculation for LiI–γ-alumina gave an energy decrease in the range 0–14 eV from site to site. This is due to the fact that the γ-alumina structure is a defective spinel and therefore the vacant tetrahedral sites are not identical.

Fig. 3 displays the Li^+–Li^+ radial distribution functions on the LiI/α-Al_2O_3 surfaces and the (001), (002) planes in the LiI crystal structure. The Li^+ ions on the α-alumina (0001) interfaces occupy tetrahedral sites. If all tetrahedral sites would be occupied, the Li^+ ions would form a two-dimensional hexagonal lattice with $|\vec{a}| = |\vec{b}| \approx 4.75$ Å as translation vectors. The peaks, denoted by A, B and C in Fig. 3, are typical for an hexagonal lattice with 4.75 and 8.35 Å as nearest neighbour and next nearest neigbour distances, respectively.

For the LiI/γ-Al_2O_3 surfaces and the (001), (002) planes of crystalline LiI, the Li^+–Li^+ RDFs are shown in Fig. 4. Here the Li^+ ions are also situated at the tetrahedral sites. On the γ-alumina (001) plane, the Li^+ ions prefer however to form a square lattice with the nearest tetrahedral site remaining vacant. However, there are some cases where the nearest tetrahedral site of a Li^+ ion is occupied as well. This results in the small peak A (≈3.0 Å) denoted in Fig. 4. Peaks B (≈5.72 Å) and C (≈8.18 Å) in Fig. 4 denote respectively the nearest and next nearest neighbour distances of the square lattice which the Li^+ ions prefer on the γ-alumina surface.

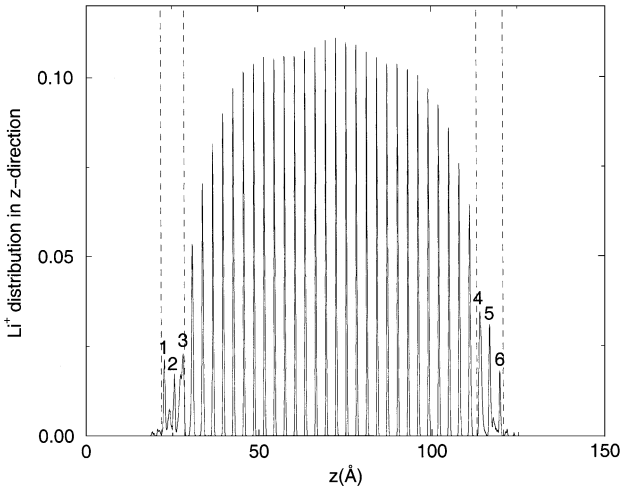

Fig. 2. Li^+ ZDF in LiI/γ-Al_2O_3 (300 K). The dashed lines denote the depleted regions while the numbers 1–6 its Li^+ layers.

3.2. Spectra

The vibrational DOS of the Li^+ ions in LiI/α-Al_2O_3 and LiI/γ-Al_2O_3 (Figs. 5 and 6) have been determined through a Fourier transform of the VACF.

$$\mathrm{DOS}(\nu) = \int_0^\infty \frac{<\vec{v}_i(t)\cdot\vec{v}_i(0)>}{\langle\vec{v}_i(0)\cdot\vec{v}_i(0)\rangle}\cos(2\pi\nu t)\mathrm{d}t. \qquad (1.3)$$

Here ν is the frequency and $\vec{v}_i(t)$ the velocity of particle i at time t. The Li^+ ion spectra in pure LiI have been included for comparison in the figures. The spectra reveal a shift to the left by ≈ 50 cm^{-1} for LiI/α-Al_2O_3 and ≈ 20 cm^{-1} for LiI/γ-Al_2O_3. This could be a consequence of the change of the long-range electrostatic potential caused by the presence of alumina crystals which reduce the frequency of the vibrations of the Li^+ ions in the LiI crystal structure. The Li^+ ions in the interfaces have one broad band 180–450 cm^{-1} indicating the absence of a well-defined potential well. Similar behaviour was observed at higher temperatures.

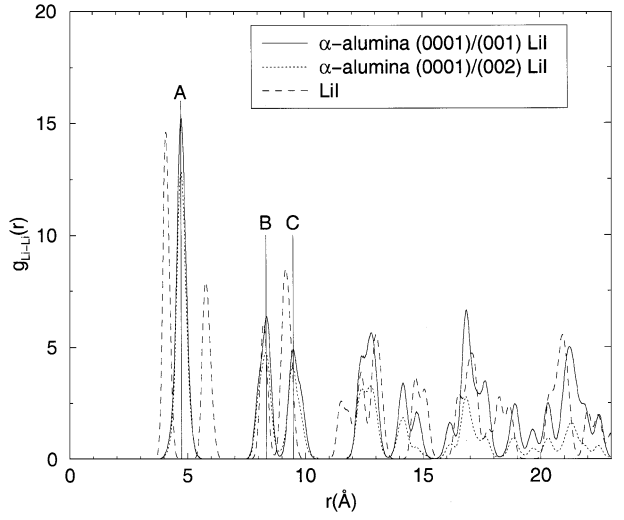

Fig. 3. Li^+–Li^+ RDF (300 K) in LiI/α-Al_2O_3 of the Li^+ ions with the same z value in the two α-alumina surfaces and the bulk.

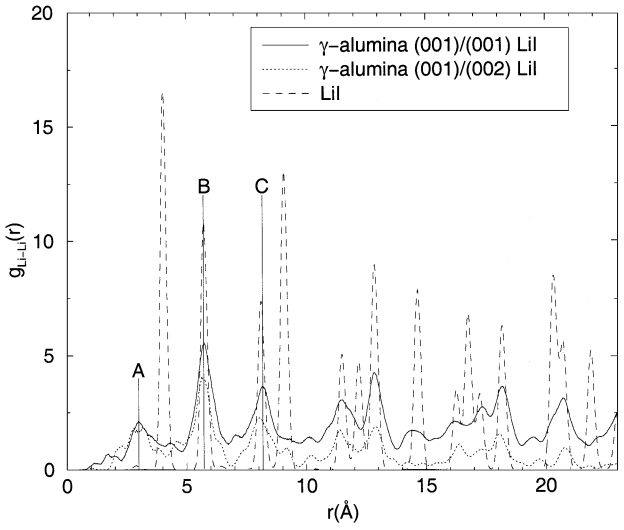

Fig. 4. Li^+–Li^+ RDF (300 K) in LiI/γ-Al_2O_3 of the Li^+ ions with the same z value in the two γ-alumina surfaces and the bulk.

3.3. Space charge

Enhanced ionic conductivity in many nanocomposites has been explained by the space charge model. In this model, the formation of space charge regions is suggested which induce strong local electric fields in the interfaces. These electric fields then give rise to the enhanced self-diffusion. We have measured the average total electric field function (EF) over 0.1 ns as a function of the position z in the [001] direction perpendicular to the interface as

$$\mathrm{EF}(z) = \left|\left\langle \sum_i \vec{E}_i(x,y,z)\delta(z-z_i)\right\rangle\right|. \qquad (1.4)$$

Here $\vec{E}_i(x,y,z)$ is the electric field acting on i. To decrease the fluctuations in the curves, running averages of the

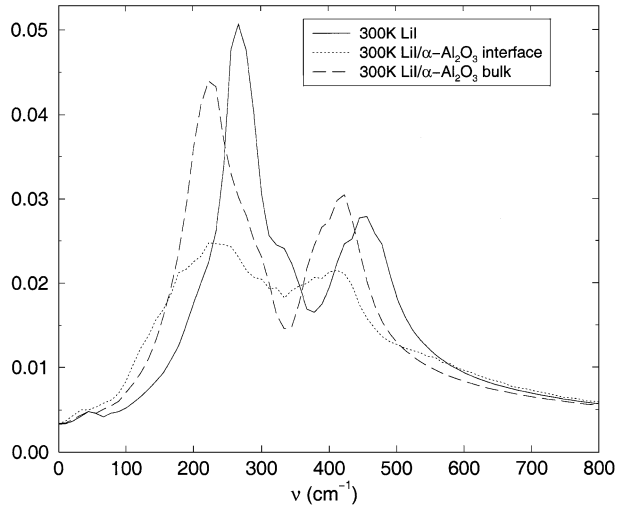

Fig. 5. DOS of the Li^+ ions in LiI/α-Al_2O_3 and LiI.

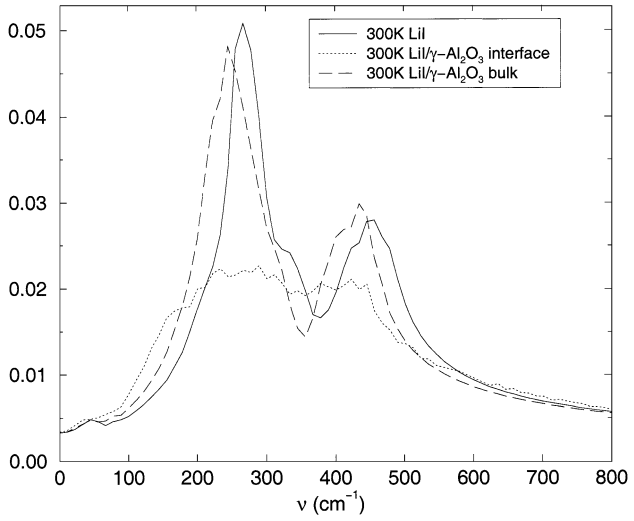

Fig. 6. DOS of the Li^+ ions in LiI/γ-Al_2O_3 and LiI.

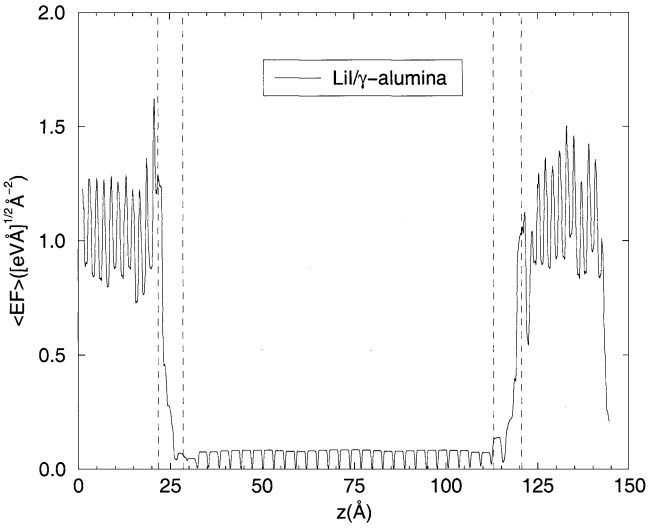

Fig. 8. LiI/γ-Al_2O_3 (300 K). The dashed lines indicate the interface regions.

electric field ⟨EF⟩ were taken. For LiI/α-alumina, the EF is depicted in Fig. 7. Fig. 7 clearly shows an enhanced electric field at both interfaces in the LiI/α-alumina sample. This is caused by the layer of Li^+ ions which are attached at the α-alumina surfaces. Since the density of Li^+ ions attached to the γ-alumina surfaces is lower, the enhancement of the electric field in the LiI/α-alumina interfaces is smaller and can hardly be noticed in Fig. 8. Measurements of the EFs in the directions parallel to the interfaces gave no enhanced electric field in the LiI/α,γ-alumina samples.

3.4. Diffusion

We have measured the mean square displacement (MSD) of the Li^+ ions separately in the bulk and along the interfaces in respectively LiI/α-Al_2O_3 and LiI/γ-Al_2O_3. No diffusion could be measured in the bulk. The diffusion coefficients, D, were obtained from the MSD by using Einstein's relation,

$$D = \frac{1}{4}\lim_{t\to\infty}\frac{\mathrm{d}}{\mathrm{d}t}\left(\frac{1}{N}\sum_{i=1}^{N}\left\langle\left[\vec{r}_i(t)-\vec{r}_i(0)\right]^2\right\rangle\right), \qquad (1.5)$$

where N is the total number of Li^+ ions and the two-dimensional nature of diffusion have been taken into account. Arrhenius plots of D are depicted in Fig. 9. The activation energies in the interfaces are all of the same order ($E_a \approx 0.38$ eV). In all the interfaces, diffusion is indirectly caused by the Li^+ ions that have moved to the alumina surface creating vacant sites in the layers 2, 3, 5 and 6 (Figs. 1 and 2). The Li^+ ions in the layers 2, 3, 5 and 6 become mobile in the presence of those vacant sites. Therefore the diffusion mechanism in LiI/α-alumina and LiI/γ-alumina is the same explaining the equality of the activation energies for diffusion in both interfaces.

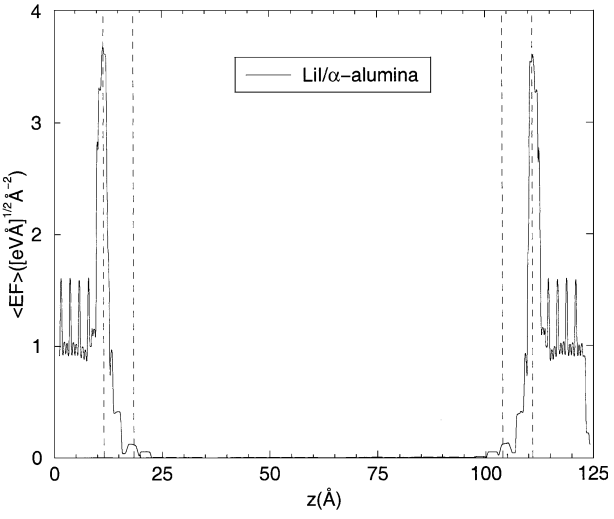

Fig. 7. EF of LiI/α-Al_2O_3 (300 K). The dashed lines denote the interface regions.

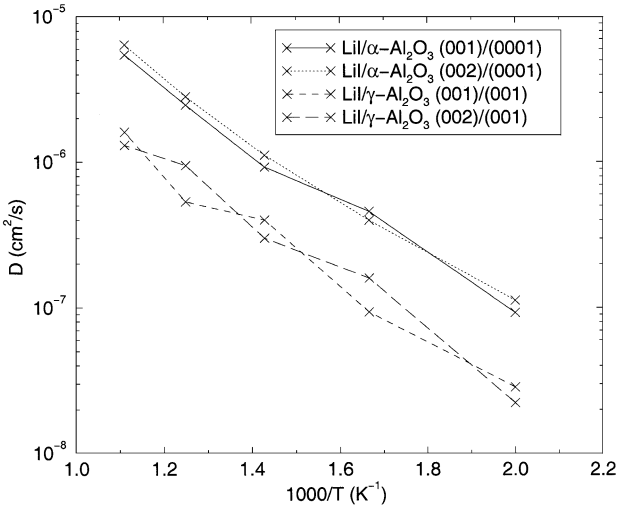

Fig. 9. Arrhenius plot of Li^+ ions in the interfaces. The crosses denote the measured data points.

The prefactors, D_o, are $\sim 7.41 \times 10^{-4}$ and $\sim 2.14 \times 10^{-4}$ cm^2/s for respectively LiI/α-Al_2O_3 and LiI/γ-Al_2O_3. The higher D_o value for LiI/α-Al_2O_3 is due to the higher number of charge carriers compared to LiI/γ-Al_2O_3.

4. Conclusions

Molecular dynamics simulations were performed on LiI/α,γ-alumina. The simulations show that the conductivity of the Li^+ is increased when it is mixed with α- or γ-alumina.

Diffusion was found to take place mainly along the interfaces LiI (001),(002)/α-Al_2O_3 (0001) and LiI (001),(002)/γ-Al_2O_3 (001) formed by the alumina and the LiI crystal planes. A fraction of Li^+ ions was found to move to the alumina surfaces. On both (0001) α-alumina and (001) γ-alumina surfaces, the Li^+ ions reside in vacant tetrahedral sites. On the (0001) α-alumina surface, the RDF reveals that the Li^+ ions form a hexagonal lattice while at the γ-alumina surface they form a square lattice. The distribution of the Li^+ along the [001] direction confirms the fact that the Li^+ ions have partly moved to the alumina surface. The average number of density of Li^+ ions on the α-alumina surface (0.0277 $Å^{-2}$) was larger than at the γ-alumina surface (0.0196 $Å^{-2}$).

An enhanced electric field was clearly found at the LiI/α-alumina interface. This was less clear for the LiI/γ-alumina interfaces because of the lower number of Li^+ ions attached to the γ-alumina surfaces. The electric field was found to be along the [001] direction and therefore it has no direct influence on the conductivity.

The DOS of the Li^+ ions in the LiI and LiI/α,γ-alumina crystal were determined. Two bands could be found for the Li^+ ions in the crystal structure while only one broad band was obtained for those in the interfaces. This is due to the absence of a well-defined potential well in the interface. The presence of the alumina crystal leads to a reduction of the frequency of oscillations of the Li^+ ions.

The motion of the Li^+ ions to the alumina surfaces creates vacant sites in the LiI crystal increasing the conductivity. Since the number of Li^+ ions on the γ-alumina surfaces is lower than at the α-alumina surfaces, the diffusion coefficient is also lower. The diffusion mechanism is however the same and the activation energies for diffusion were therefore roughly identical (≈ 0.38 eV), the difference in diffusion coefficient being the result of different prefactors.

Acknowledgements

This work has been supported by FOM, Stichting voor Fundamenteel Onderzoek der Materie. The authors would like to thank NCF for generously providing computing time on the TERAS Origin 3800 at SARA (Amsterdam).

References

[1] C.C. Liang, J. Electrochem. Soc. 120 (1973) 1289.
[2] J.B. Phipps, D.L. Johnson, D.H. Whitmore, Solid State Ion. 5 (1981) 393.
[3] F.W. Poulsen, N.H. Andersen, B. Kindl, J. Schoonman, Solid State Ion. 9 and 10 (1983) 119.
[4] T. Jow, J.B. Wagner Jr., J. Electrochem. Soc. 126 (1979) 1963.
[5] J. Maier, Phys. Status Solidi, B 123 (1984) K89.
[6] J. Maier, Solid State Ion. 23 (1987) 59.
[7] J. Maier, Phys. Status Solidi, A 112 (1989) 115.
[8] N.J. Dudney, J. Am. Ceram. Soc. 68 (1985) 538.
[9] D. Lubben, F.A. Modine, J. Appl. Phys. 80 (1996) 5150.
[10] J. Deppe, M. Balkanski, R.F. Wallis, A.R. McGurn, Phys. Rev., B 45 (1992) 5687.
[11] S. Blonski, S.H. Garofalini, Surf. Sci. 295 (1993) 263.
[12] S. Blonski, S.H. Garofalini, Catal. Lett. 25 (1994) 325.
[13] J.V.L. Beckers, C.P. Lowe, S.W. de Leeuw, Mol. Simul. 20 (1998) 369.